

# Distribution-free stochastic model updating of dynamic systems with parameter dependencies

Masaru Kitahara<sup>a,\*</sup>, Sifeng Bi<sup>b</sup>, Matteo Broggi<sup>a</sup>, Michael Beer<sup>a,c,d</sup>

<sup>a</sup> Leibniz Universität Hannover, Institute for Risk and Reliability, Hannover, Germany

<sup>b</sup> University of Strathclyde, Department of Mechanical & Aerospace Engineering, Aerospace Centre of Excellence, Glasgow, United Kingdom

<sup>c</sup> University of Liverpool, Institute for Risk and Uncertainty, Liverpool, United Kingdom

<sup>d</sup> Tongji University, International Joint Research Center for Engineering Reliability and Stochastic Mechanics, Shanghai, China

\* Correspondence author. E-mail address: masaru.kitahara@irz.uni-hannover.de (M. Kitahara).

**Abstract:** This work proposes a distribution-free stochastic model updating framework to calibrate the joint probabilistic distribution of the multivariate correlated parameters. In this framework, the marginal distributions are defined as the staircase density functions and the correlation structure is described by the Gaussian copula function. The first four moments of the staircase density functions and the correlation coefficients are updated by an approximate Bayesian computation, in which the Bhattacharyya distance-based metric is proposed to define an approximate likelihood that is capable of quantifying the discrepancy between model outputs and measurement data. The feasibility of the framework is demonstrated on two illustrative examples and a followed real-world application to a nonlinear dynamic system updating problem based on measured time signals. The results indicate the importance of considering the parameter dependencies in stochastic model updating.

## Keywords:

Uncertainty quantification; Bayesian model updating; Staircase density function; Gaussian copula function; Bhattacharyya distance

## 1. Introduction

The model updating has been developed as a fascinating technique to mitigate the discrepancy between model outputs and experimental measurements [1,2]. The causes of the discrepancy during the model updating can be generally classified into following three categories:

- Parameter uncertainty. Model parameters, e.g., geometry dimensions, boundary conditions, and material properties, often cannot be exactly determined;
- Modelling uncertainty. Simplifications or approximations, e.g., linearization and frictionless mechanical joints, have to be made to numerically represent the physical system;
- Measurement uncertainty. Measured quantities are inevitably contaminated by the hard-to-control randomnesses, e.g., environmental noises and measurement system errors.

The deterministic model updating, especially for the sensitivity method [1], might be one of the most successful model updating techniques. It aims at calibrating the model parameters to find their optimal values from a single set of measurements. It has been employed in a wide range of practical applications, including the correction of large-scale finite element (FE) models [3,4]. Nevertheless, it accounts for measurement data as an exactly determined values/signals, with no consideration of the measurement uncertainty.

Comparatively, the stochastic model updating, including the perturbation method [5,6], Monte Carlo method [7,8], and Bayesian method [2,9], can be interpreted as the techniques to calibrate not the parameters themselves but the uncertainty characteristics, i.e., probabilistic distributions, so that the model outputs are committed not to the maximum fidelity to a single set of measurements but to the uncertainty characteristics of the multiple sets of measurements. In the stochastic model updating,

46 uncertainty quantification (UQ) metrics play a key role to quantify the statistical discrepancy between  
47 the model outputs and measurements because of the above three sources of uncertainty. A series of  
48 distances, such as the Euclidian distance, Mahalanobis distance, and Bhattacharyya distance has been  
49 successfully proposed to define the UQ metrics in the stochastic model updating [8]. In addition, the  
50 Frobenius norm has been also utilized to define the UQ metric to quantify the difference between the  
51 covariance matrices of the model outputs and measurements [10]. Bi et al. [11] has recently developed  
52 a Bayesian updating framework employing the approximate Bayesian computation (ABC) technique  
53 [12,13], where the Bhattacharyya distance-based approximate likelihood is used. This framework has  
54 been demonstrated to be capable to calibrate numerical models such that the model outputs recreate  
55 wholly the uncertainty characteristics of target measurements. The framework has been furthermore  
56 extended to the calibration of dynamic systems, so that the procedure enables to quantify wholly the  
57 uncertainty characteristics of the measured time signals [14].

58 In the stochastic model updating, distribution families of the parameters commonly need to be  
59 assigned a priori, then the prior distribution of the hyper-parameters such as means and variances is  
60 updated to the posterior distribution using the measurement data. The distribution families, however,  
61 are often unknown beforehand due to the scarce and/or incomplete available data for the parameters.  
62 The newly released NASA UQ challenge problem 2019 [15], for instance, requires a model calibration  
63 task in an extremely challenging condition that no distribution information of the aleatory parameters  
64 is provided other than a common bounded support domain. In such situation, the assumption on the  
65 distribution formats might significantly affect the model updating results. Therefore, Kitahara et al.  
66 [16] has recently developed a distribution-free Bayesian updating framework, where staircase density  
67 functions [17] are assigned to the underlying distribution families of the parameters. Staircase density  
68 functions enable to flexibly approximate a broad range of distributions arbitrary close, such as highly  
69 skewed and/or multi-modal distributions, and are hence particularly appropriate to characterize the  
70 parameters whose density formats cannot be specified. The framework has been demonstrated to be  
71 capable to calibrate the probabilistic distribution of the parameters without limiting hypotheses upon  
72 the distribution families.

73 Nevertheless, the aforementioned distribution-free updating framework still has open questions.  
74 Firstly, the framework has been currently only demonstrated on the updating by scalar-valued modal  
75 responses. Hence, in this study, it is extended to the updating of dynamic systems by measured time  
76 signals. Secondly, staircase density functions are provided for univariate random variables, and thus  
77 cannot consider the parameter dependencies, which might lead to inaccurate updating results in the  
78 presence of strong correlation among parameters. Copula functions are well-known to be capable to  
79 provide an effective way to characterize the dependence structure among parameters, and have been  
80 widely applied to reliability problems [18-20]. Among various types of copula functions, the Gaussian  
81 copula function is most widely used because it can be easily generalized to the multivariate case, and  
82 this property is particularly attractive for the stochastic model updating problem, in which very large  
83 number of parameters is considered as random variables.

84 The objective of this work is consequently to develop a stochastic model updating framework to  
85 calibrate the joint probability distribution of the correlated parameters without prior knowledge on  
86 the distribution families of the marginal distributions. In order to achieve this task, it is assumed that  
87 the joint probability distribution of the parameters is characterized by a combination of the Gaussian  
88 copula function and staircase density functions. Moment constraints for the existence of the staircase  
89 density functions and the correlation coefficient constraint for the existence of the copula function are  
90 then derived. Furthermore, the Bhattacharyya distance is utilized to define an approximate likelihood  
91 function quantifying the stochastic discrepancy between the model outputs and measurements, such  
92 that the hyper-parameters of the staircase density functions as well as the correlation coefficients of  
93 the copula function are calibrated through an ABC updating approach. The proposed framework is  
94 first demonstrated on both bi-variate and multi-variate cases using two simple illustrative examples,  
95 and then applied to a model updating problem of a seismic-isolated bridge pier model based on the  
96 simulated seismic response data, so as to demonstrate the feasibility of the framework in the updating  
97 of nonlinear dynamic systems.

98 The structure of this paper is as follows. Section 2 first describes theoretical and methodological  
 99 bases of the three key ingredients of the proposed framework, i.e., the Bhattacharyya distance-based  
 100 UQ metrics, staircase density functions, and Gaussian copula function. Then, in Section 3, we outline  
 101 the formulation of the Bayesian updating with the combination of the Gaussian copula function and  
 102 staircase density functions, and the proposed ABC updating framework. Illustrative applications are  
 103 provided in Section 4, employing a simple shear building model and a spring-mass system, and the  
 104 feasibility of the proposed framework in the updating of nonlinear dynamic systems by the measured  
 105 time signals is further demonstrated in Section 5. Finally, Section 6 gives conclusions to this paper.

## 106 2. Theories and methodologies

### 107 2.1. Bhattacharyya distance-based UQ metrics

108 The system under investigation in the stochastic model updating is described as:

$$\mathbf{y} = h(\mathbf{x}) \quad (1)$$

109 where  $\mathbf{x} = [x_1, x_2, \dots, x_n]$  denotes a row vector of  $n$  input parameters;  $\mathbf{y} = [y_1, y_2, \dots, y_m]$  means a row  
 110 vector of  $m$  output features;  $h(\cdot)$  means the simulator. The output features herein can be either scalar-  
 111 valued modal responses or time signals. In the latter case,  $\mathbf{y}$  is replaced to be  $\mathbf{y} = [\mathbf{y}_1, \mathbf{y}_2, \dots, \mathbf{y}_m]$ , with  
 112  $\mathbf{y}_i = [y_i(0), y_i(1), \dots, y_i(t)]^T, \forall i = 1, 2, \dots, m$ , where  $t$  indicates the time parameter. The simulator  $h(\cdot)$   
 113 can be either high-fidelity models, e.g., FE models, or approximated surrogate models.

114 Uncertainties involved in the system are first characterized by representing the input parameters  
 115 as random variables, and are then propagated through the simulator to the output features. This can  
 116 be typically achieved by randomly generating the multiple sets of the parameters and corresponding  
 117 output features. Let the sample size be  $N_{\text{sim}}$ , the simulator  $h$  is evaluated  $N_{\text{sim}}$  times for obtaining the  
 118 sample set of the simulated features  $\mathbf{Y}_{\text{sim}} \in \mathbb{R}^{N_{\text{sim}} \times m}$ :

$$\mathbf{Y}_{\text{sim}} = [\mathbf{y}^{(1)}, \mathbf{y}^{(2)}, \dots, \mathbf{y}^{(N_{\text{sim}})}]^T, \text{ with } \mathbf{y}^{(k)} = [y_1^{(k)}, y_2^{(k)}, \dots, y_m^{(k)}], \forall k = 1, 2, \dots, N_{\text{sim}} \quad (2)$$

119 in the case that the output features are given as the modal responses.  $\mathbf{Y}_{\text{sim}}$  can be simply extended to  
 120  $\mathbf{Y}_{\text{sim}} \in \mathbb{R}^{N_{\text{sim}} \times m \times (t+1)}$  for the time signals case.

121 In addition to the simulated features, corresponding observed features are also necessary in the  
 122 model updating. Let the number of observations be  $N_{\text{obs}}$ , the sample set of the observed features  $\mathbf{Y}_{\text{obs}}$   
 123 possesses a same structure as Eq. (2), but only the number of rows is changed from  $N_{\text{sim}}$  to  $N_{\text{obs}}$ . The  
 124 stochastic model updating is then aimed at minimizing the stochastic discrepancy between  $\mathbf{Y}_{\text{sim}}$  and  
 125  $\mathbf{Y}_{\text{obs}}$  by calibrating the joint probability distribution of the parameters.

126 To quantify the discrepancy between  $\mathbf{Y}_{\text{sim}}$  and  $\mathbf{Y}_{\text{obs}}$ , the Bhattacharyya distance-based UQ metric  
 127 is employed in this study. The original definition of the Bhattacharyya distance is given as [21]:

$$d_B(\mathbf{Y}_{\text{sim}}, \mathbf{Y}_{\text{obs}}) = -\log \left[ \int_{\mathbf{y}} \sqrt{f_{\mathbf{Y}_{\text{sim}}}(\mathbf{y}) f_{\mathbf{Y}_{\text{obs}}}(\mathbf{y})} d\mathbf{y} \right] \quad (3)$$

128 where  $f_{(\cdot)}(\mathbf{y})$  means the probability density function (PDF) of the output features  $\mathbf{y}$ ;  $\mathbf{y}$  is the support  
 129 domain of the output features which comprises  $m$ -dimensional space for the modal responses but the  
 130  $\{m \times (t+1)\}$ -dimensional space for the time signals. Eq. (3) indicates the Bhattacharyya distance is a  
 131 measure of the overlap between the two probability distributions. Hence, it is capable to consider not  
 132 only mean information but whole statistical information of two different sample sets. However, the  
 133 direct evaluation of Eq. (3) is usually impractical since precisely estimating the joint PDF of the output  
 134 features is non-trivial due to the necessity of time-consuming repeated model evaluations or the very  
 135 limited number of available measurement data. To overcome this issue, Bi et al. [11] proposes the so-  
 136 called binning algorithm to evaluate the probability mass function (PMF) of the given sample sets, so  
 137 that the discrete Bhattacharyya distance is utilized instead [22]:

$$d_B(\mathbf{Y}_{\text{sim}}, \mathbf{Y}_{\text{obs}}) = -\log \left\{ \sum_{j=1}^{N_{\text{bin}}} \sqrt{P_{\mathbf{Y}_{\text{sim}}}^{(j)} P_{\mathbf{Y}_{\text{obs}}}^{(j)}} \right\} \quad (4)$$

138 where  $N_{\text{bin}}$  denotes the total number of bins;  $P_{(\cdot)}^{(j)}$  denotes the PMF value of the output features at the  
 139  $j$ th bin. In the binning algorithm, a grid is created in the whole support domain of the output features,  
 140 and thus the total number of bins would be  $N_{\text{bin}} = n_{\text{bin}}^m$  for the modal responses and  $N_{\text{bin}} = n_{\text{bin}}^{m \times (t+1)}$   
 141 for the time signals, where  $n_{\text{bin}}$  indicates the number of bins for each output feature. One can refer to  
 142 Ref. [11] for the detailed procedure of the binning algorithm. The discrete Bhattacharyya distance has  
 143 been demonstrated to be effective in relatively low-dimensional problems (e.g., the dimension is less  
 144 than six).

145 On the other hand, even the evaluation of Eq. (4) is still impractical for the very high-dimensional  
 146 problems where the output features comprise time signals, since the number of bins is exponentially  
 147 increasing with the number of dimensions because of the so-called curse of dimensionality. To tackle  
 148 this issue, Kitahara et al. [14] proposes a dimension reduction procedure to employ the Bhattacharyya  
 149 distance for the comparison of two different time signals, consisting of the following steps:

- 150 1) Define the common window length  $L$  for  $\mathbf{Y}_{\text{sim}}$  and  $\mathbf{Y}_{\text{obs}}$ . Divide them into three-dimensional  
 151 sub-arrays  $\mathbf{Y}_{\text{sim}}^s \in \mathbb{R}^{N_{\text{sim}} \times m \times L}$  and  $\mathbf{Y}_{\text{obs}}^s \in \mathbb{R}^{N_{\text{obs}} \times m \times L}$ ,  $\forall s = 1, \dots, \lfloor (t+1)/L \rfloor$ , where  $\lfloor \cdot \rfloor$  denotes  
 152 the lower integer of the investigated values;
- 153 2) Compute the root mean square (RMS) matrices  $\mathbf{R}_{\mathbf{Y}_{\text{sim}}^s} \in \mathbb{R}^{N_{\text{sim}} \times m}$  of each sub-array  $\mathbf{Y}_{\text{sim}}^s$  along  
 154 its third dimension and obtain the sample set of the RMS values  $\mathbf{R}_{\mathbf{Y}_{\text{sim}}} \in \mathbb{R}^{N_{\text{sim}} \times m \times \lfloor (t+1)/L \rfloor}$ . Do  
 155 similar procedure for the observed features and obtain  $\mathbf{R}_{\mathbf{Y}_{\text{obs}}} \in \mathbb{R}^{N_{\text{obs}} \times m \times \lfloor (t+1)/L \rfloor}$ ;
- 156 3) Evaluate in total  $\lfloor (t+1)/L \rfloor$  Bhattacharyya distances  $d_B^s$  between two sample sets  $\mathbf{R}_{\mathbf{Y}_{\text{sim}}^s}$  and  
 157  $\mathbf{R}_{\mathbf{Y}_{\text{obs}}^s}$  using Eq. (4);
- 158 4) Employ the RMS value of the set of the Bhattacharyya distances,  $R_{d_B}$ , as the UQ metric.

159 The authors' experience shows that  $L = (0.02 \sim 0.03) \cdot t$  is the reasonable choice for the window length  
 160  $L$ , and such choice indicates that each window contains 2~3 % of the time signals. As such, the time  
 161 signals are degraded to a series of RMS values, the above defined Bhattacharyya distance-based UQ  
 162 metric has been demonstrated to be able to quantify the uncertainty characteristics of the entire time  
 163 signals [14].

## 164 2.2. Staircase density functions

165 Let the input parameter  $x_i$ ,  $\forall i = 1, \dots, n$ , be a random variable having the support domain  $[\underline{x}_i, \bar{x}_i]$   
 166 and a quadruple of the hyper-parameters  $\boldsymbol{\theta}_{x_i} = [\mu_i, m_{2i}, \tilde{m}_{3i}, \tilde{m}_{4i}]$  consisting of the mean  $\mu_i$ , variance  
 167  $m_{2i}$ , skewness  $\tilde{m}_{3i}$ , and kurtosis  $\tilde{m}_{4i}$ . The skewness  $\tilde{m}_{3i}$  and kurtosis  $\tilde{m}_{4i}$  are defined as ratios of the  
 168 variance to the third and fourth central moments by  $\tilde{m}_{3i} = m_{3i}/m_{2i}^{3/2}$  and  $\tilde{m}_{4i} = m_{4i}/m_{2i}^2$ , respectively.  
 169 The feasibility condition for the existence of  $x_i$  can be defined as moment constraints given by a series  
 170 of inequalities  $\Theta_i = \{\boldsymbol{\theta}_{x_i} : g(\boldsymbol{\theta}_{x_i}) \leq 0\}$ , and their components are summarized in Table 1 [23,24].

171 **Table 1.** Moment constraints for the existence of staircase density functions.

Hyper-parameters	Moment constraints
Mean $\mu_i$	$g_1 = \underline{x}_i - \mu_i$ $g_2 = \mu_i - \bar{x}_i$
Variance $m_{2i}$	$g_3 = -m_{2i}$ $g_4 = m_{2i} - v_i$
Skewness $\tilde{m}_{3i}$	$g_5 = m_{2i}^2 - m_{2i}(\mu_i - \underline{x}_i)^2 - \tilde{m}_{3i}m_{2i}^{3/2}(\mu_i - \underline{x}_i)$ $g_6 = \tilde{m}_{3i}m_{2i}^{3/2}(\bar{x}_i - \mu_i) - m_{2i}(\bar{x}_i - \mu_i)^2 + m_{2i}^2$ $g_7 = 4m_{2i}^2 + \tilde{m}_{3i}^2m_{2i}^3 - m_{2i}^2(\bar{x}_i - \underline{x}_i)^2$ $g_8 = 6\sqrt{3}\tilde{m}_{3i}m_{2i}^{3/2} - (\bar{x}_i - \underline{x}_i)^3$ $g_9 = -6\sqrt{3}\tilde{m}_{3i}m_{2i}^{3/2} - (\bar{x}_i - \underline{x}_i)^3$
Kurtosis $\tilde{m}_{4i}$	$g_{10} = -\tilde{m}_{4i}m_{2i}^2$ $g_{11} = 12\tilde{m}_{4i}m_{2i}^2 - (\bar{x}_i - \underline{x}_i)^4$ $g_{12} = (\tilde{m}_{4i}m_{2i}^2 - v_im_{2i} - u_i\tilde{m}_{3i}m_{2i}^{3/2})(v_i - m_{2i}) + (\tilde{m}_{3i}m_{2i}^{3/2} - \mu_im_{2i})^2$ $g_{13} = \tilde{m}_{3i}^2m_{2i}^3 + m_{2i}^3 - \tilde{m}_{4i}m_{2i}^3$

<sup>a</sup>  $u_i = \underline{x}_i + \bar{x}_i - 2\mu_i$  and  $v_i = (\mu_i - \underline{x}_i)(\bar{x}_i - \mu_i)$ .

172 Let the bounded support domain  $[x_i, \bar{x}_i]$  equally partitioned into  $n_b$  subintervals with the length  
 173  $\kappa = (\bar{x}_i - x_i)/n_b$ ,  $x_i$  can be considered as a staircase random variable, and then its PDF  $f_{x_i}(x)$  can be  
 174 expressed as [17]:

$$f_{x_i}(x) = \begin{cases} l^j & \forall x \in (x_i^j, x_i^{j+1}], \forall j = 1, 2, \dots, n_b \\ 0 & \text{otherwise} \end{cases} \quad (5)$$

175 where  $l^j$  is the PDF value of the  $j$ th bin;  $x_i^j = x_i + (j - 1)\kappa$  is the left partitioning point of the  $j$ th bin.  
 176 It is noted that  $l^j$  holds that  $l^j \geq 0$  for all the bins and  $\kappa \sum_{j=1}^{n_b} l^j = 1$ . The PDF values  $l_i$  are obtained by  
 177 solving the following optimization problem [17]:

$$\hat{l}_i = \underset{l \geq 0}{\operatorname{argmin}} \left\{ J(\mathbf{l}): \sum_{j=1}^{n_b} \int_{x_i^j}^{x_i^{j+1}} x l^j dx = \mu_i, \sum_{j=1}^{n_b} \int_{x_i^j}^{x_i^{j+1}} (x - \mu_i)^r l^j dx = m_{r_i}, r = 2, 3, 4 \right\} \quad (6)$$

178 where  $J(\cdot)$  is an arbitrary selected cost function expressed as:

$$J(\mathbf{l}) = \mathbf{l}^T \mathbf{I} \mathbf{l} \quad (7)$$

179 where  $\mathbf{I}$  means the identity matrix. This cost function leads to the resultant staircase random variables  
 180 minimizing the squared sum of the likelihood at each bin. Based on the moment matching constraints,  
 181 Eq. (6) can be written as [17]:

$$\hat{l}_i = \underset{l \geq 0}{\operatorname{argmin}} \{ J(\mathbf{l}): \mathbf{A}(\theta_{x_i}, n_b) \mathbf{l} = \mathbf{b}(\theta_{x_i}), \theta_{x_i} \in \Theta_i \} \quad (8)$$

182 where

$$\mathbf{A} = \begin{bmatrix} \kappa \mathbf{e} \\ \kappa \mathbf{c} \\ \kappa \mathbf{c}^2 + \kappa^3/12 \\ \kappa \mathbf{c}^3 + \kappa^3 \mathbf{c}/4 \\ \kappa \mathbf{c}^4 + \kappa^3 \mathbf{c}^2/2 + \kappa^5/80 \end{bmatrix}, \text{ and } \mathbf{b} = \begin{bmatrix} 1 \\ \mu_i \\ \mu_i^2 + m_{2i} \\ \tilde{m}_{3i} m_{2i}^{3/2} + 3\mu_i m_{2i} + \mu_i^3 \\ m_{4i} m_{2i}^2 + 4\tilde{m}_{3i} m_{2i}^{3/2} \mu_i + 6m_{2i} \mu_i^2 + \mu_i^4 \end{bmatrix}$$

183 where  $\mathbf{c}$  means a column vector of the centre of the bin  $c_j = (x_i^j + x_i^{j+1})/2$ ;  $\mathbf{c}^n$  denotes the component  
 184 wise  $n$ th power of  $\mathbf{c}$ ;  $\mathbf{e}$  refers to a vector of ones.

185 The convexity of the optimization problem in Eq. (8) enables the fast computation of the staircase  
 186 density heights. In addition, a relatively small value of  $n_b$  (e.g.,  $n_b = 25 \sim 50$ ) is enough for obtaining  
 187 practically smooth distribution shapes for the PMF evaluation, which makes the computation further  
 188 faster. These features are particularly appropriate for the stochastic updating, where the tremendous  
 189 number of computations of the probability distributions is necessary. Furthermore, staircase density  
 190 functions enable to flexibly approximate a broad range of distributions arbitrary close, such as highly  
 191 skewed and/or multi-modal distributions. Therefore, they can serve as a distribution-free uncertainty  
 192 characterization model of the parameters whose distribution families cannot be determined.

### 193 2.3. Gaussian copula function

194 Copula functions couple the multivariate joint cumulative distribution function (CDF) with its  
 195 one-dimensional marginal CDFs. Conversely, copula functions are also seen as the multivariate joint  
 196 CDFs whose one-dimensional marginal CDFs follow a uniform distribution on the interval of  $[0, 1]$ .  
 197 According to Sklar's theorem [25], the bivariate joint CDF of two random variables  $x_1$  and  $x_2$  can be  
 198 expressed as:

$$F_{\mathbf{x}}(x_1, x_2) = C(F_{x_1}(x_1), F_{x_2}(x_2)) \quad (9)$$

199 where  $F_{x_1}(x_1)$  and  $F_{x_2}(x_2)$  are the marginal CDFs of  $x_1$  and  $x_2$ , respectively;  $C(F_{x_1}(x_1), F_{x_2}(x_2))$  is the  
 200 copula function. From Eq. (9), the bivariate joint PDF of  $x_1$  and  $x_2$  is then written as:

$$f_{\mathbf{x}}(x_1, x_2) = c(F_{x_1}(x_1), F_{x_2}(x_2)) f_{x_1}(x_1) f_{x_2}(x_2) \quad (10)$$

201 where  $c(F_{x_1}(x_1), F_{x_2}(x_2))$  denotes the copula density function given as:

$$c(F_{x_1}(x_1), F_{x_2}(x_2)) = c(u_1, u_2) = \frac{\partial^2 c(u_1, u_2)}{\partial u_1 \partial u_2} \quad (11)$$

202 Theoretically, the joint distribution of  $x_1$  and  $x_2$  can be fully and uniquely represented by Eqs. (9) and  
203 (10) if the marginal distributions of  $x_1$  and  $x_2$ , and the copula function are given.

204 There are many copula function types in the literature, including the Gaussian, t, Frank, Gumbel,  
205 and Clayton copula functions. They are characterized by their own dependence structures. The latter  
206 three types of copula function can be referred to as Archimedean copulas. The Archimedean copulas  
207 have only a single parameter, and thus cannot provide the general dependence structure among more  
208 than two random variables. Alternatively, the general dependence structure is often modeled by the  
209 pair-copula decomposition introduced as a canonical vine copula [26]. Conversely, the Gaussian and  
210 t copulas, which belong to elliptical copulas, can be straightforwardly generalized to the multivariate  
211 case. Particularly, the Gaussian copula function is most widely used since it only needs the correlation  
212 matrix to determine the dependence structure.

213 In this study, the joint probability distribution of the input parameters  $\mathbf{x}$  is finally characterized  
214 by the combination of the Gaussian copula function and staircase density functions as:

$$\begin{aligned} F_{\mathbf{x}}(\mathbf{x}) &= C_G(F_{x_1}(x_1), F_{x_2}(x_2), \dots, F_{x_n}(x_n); \boldsymbol{\rho}) \\ &= \Phi_{\boldsymbol{\rho}}\left(\Phi^{-1}(F_{x_1}(x_1)), \Phi^{-1}(F_{x_2}(x_2)), \dots, \Phi^{-1}(F_{x_n}(x_n))\right) \end{aligned} \quad (12)$$

215 where  $C_G$  indicates the Gaussian copula function;  $\boldsymbol{\rho}$  indicates the correlation matrix;  $\Phi_{\boldsymbol{\rho}}$  indicates the  
216 multivariate standard normal CDF with  $\boldsymbol{\rho}$ ;  $\Phi^{-1}$  indicates the inverse function of the standard normal  
217 CDF. It is noted that each marginal CDF  $F_{x_i}(x_i)$  can be described by the empirical CDF of the staircase  
218 density function  $f_{x_i}(\cdot)$ , for  $i = 1, 2, \dots, n$ . The correlation matrix  $\boldsymbol{\rho}$  can be expressed as:

$$\boldsymbol{\rho} = \begin{bmatrix} 1 & \rho_{12} & \rho_{13} & \dots & \rho_{1n} \\ \rho_{12} & 1 & \rho_{23} & \dots & \rho_{2n} \\ \rho_{13} & \rho_{23} & \ddots & \dots & \vdots \\ \vdots & \vdots & \vdots & 1 & \rho_{n-1n} \\ \rho_{1n} & \rho_{2n} & \dots & \rho_{n-1n} & 1 \end{bmatrix} \quad (13)$$

219 where  $\rho_{ij}$ , for  $i = 1, 2, \dots, n-1$  and  $j = i+1, \dots, n$ , means the correlation coefficient. The range of each  
220 correlation coefficient can reach  $[-1, 1]$ . The correlation matrix  $\boldsymbol{\rho}$  should be the symmetric and positive  
221 semi-definite matrix. Hence, the feasibility condition for the existence of the Gaussian copula function  
222 can be defined by the correlation coefficient constraint  $\mathcal{P} = \{\boldsymbol{\rho}: \text{chol}(\boldsymbol{\rho}) \neq \emptyset\}$ , where  $\text{chol}(\cdot)$  means the  
223 Cholesky factorization.

### 224 3. Distribution-free stochastic model updating

#### 225 3.1. Bayesian model updating of the joint probabilistic distribution

226 In the proposed stochastic updating framework, the well-known Bayesian inference is utilized.  
227 It is based on the Bayes' theorem [27]:

$$P(\boldsymbol{\vartheta}|\mathbf{Y}_{\text{obs}}) = \frac{P_L(\mathbf{Y}_{\text{obs}}|\boldsymbol{\vartheta})P(\boldsymbol{\vartheta})}{P(\mathbf{Y}_{\text{obs}})} \quad (14)$$

228 where  $P(\boldsymbol{\vartheta})$  denotes the prior PDF of the parameters to be inferred  $\boldsymbol{\vartheta}$  that is determined by the initial  
229 knowledge of the system and expert judgement;  $P(\boldsymbol{\vartheta}|\mathbf{Y}_{\text{obs}})$  means the posterior PDF of  $\boldsymbol{\vartheta}$  conditional  
230 to the measurements, representing the updated knowledge of  $\boldsymbol{\vartheta}$ ;  $P(\mathbf{Y}_{\text{obs}})$  indicates the normalization  
231 factor (evidence) ensuring the integral of the posterior distribution equal to one;  $P_L(\mathbf{Y}_{\text{obs}}|\boldsymbol{\vartheta})$  indicates  
232 the likelihood function of  $\mathbf{Y}_{\text{obs}}$  that is defined as the PDF values of the measurements conditional to  
233 each instance of  $\boldsymbol{\vartheta}$ .

234 To calibrate the joint probabilistic distribution of the parameters  $\mathbf{x}$  given by Eq. (13), the hyper-  
235 parameters of the staircase density functions  $\boldsymbol{\theta}_{x_i}$ , for  $i = 1, \dots, n$ , and the correlation coefficients of the  
236 Gaussian copula function  $\rho_{ij}$ , for  $i = 1, \dots, n-1$  and  $j = i+1, \dots, n$ , are considered to be the inferred  
237 parameters  $\boldsymbol{\vartheta}$ . Based on the moment constraints  $\Theta_i$ , the support domains of  $\boldsymbol{\theta}_{x_i}$  can be determined as:

$$\mu_i \in [\underline{x}_i, \bar{x}_i], m_{2i} \in \left[0, \frac{(\bar{x}_i - \underline{x}_i)^2}{4}\right], m_{3i} \in \left[-\frac{(\bar{x}_i - \underline{x}_i)^3}{6\sqrt{3}}, \frac{(\bar{x}_i - \underline{x}_i)^3}{6\sqrt{3}}\right], m_{4i} \in \left[0, \frac{(\bar{x}_i - \underline{x}_i)^4}{12}\right] \quad (15)$$

238 It is noted that the support domains are defined not for the skewness and kurtosis but the third and  
 239 fourth central moments, since the skewness and kurtosis are conditional on the variance. On the other  
 240 hand, the support domain of  $\rho_{ij}$  is simply defined as  $[-1, 1]$ . In this study, it is assumed all parameters  
 241 to be inferred are independent. Based on these support domains with the moment constraints  $\Theta_i$  and  
 242 correlation coefficient constraint  $P$ , the prior PDF  $P(\boldsymbol{\vartheta})$  can be expressed as:

$$P(\boldsymbol{\vartheta}) = \prod_{i=1}^n P(\boldsymbol{\theta}_{x_i}) I_{\Theta_i}(\boldsymbol{\theta}_{x_i}) \cdot \prod_{i=1}^{n-1} \prod_{j=i+1}^n P(\rho_{ij}) I_P(\rho_{ij}) \quad (16)$$

243 where  $P(\boldsymbol{\theta}_{x_i})$  and  $P(\rho_{ij})$  indicate the prior PDFs of the hyper-parameters and correlation coefficients  
 244 that are chosen as the uniform distributions on their respective support domains;  $I_{\Theta_i}(\boldsymbol{\theta}_{x_i})$  denotes the  
 245 indicator function of  $\boldsymbol{\theta}_{x_i}$ , which equals to one if  $\Theta_i$  is satisfied and otherwise equals to zero;  $I_P(\rho_{ij})$  is  
 246 similarly the indicator function of  $\rho_{ij}$ . As such, the proposed stochastic updating framework requires  
 247 only assumptions on the support domains of the input parameters  $\mathbf{x}$ .

248 This brings totally  $4n + n(n-1)/2$  inferred parameters. However, it is widely recognized that  
 249 the direct evaluation of the posterior PDF over such a high-dimensional parameter space is not trivial  
 250 [28]. Hence, the well-known advanced sampling technique, termed transitional Markov chain Monte  
 251 Carlo (TMCMC) [29], is employed in this study. TMCMC is a sequential procedure sampling from a  
 252 series of transitional PDFs that will gradually converge to the actual posterior PDF, thus it enables to  
 253 generate samples from the very complex posterior PDF. One can refer to Refs. [29,30] for more details  
 254 of the TMCMC algorithm.

### 255 3.2. Approximate Bayesian computation

256 The likelihood function plays a key role in the Bayesian model updating. Utilizing the Bayesian  
 257 inference in the stochastic updating results in the following theoretical likelihood function:

$$P_L(\mathbf{Y}_{\text{obs}}|\boldsymbol{\vartheta}) = \prod_{k=1}^{N_{\text{obs}}} P(\mathbf{Y}_{\text{obs}}^{(k)}|\boldsymbol{\vartheta}) \quad (17)$$

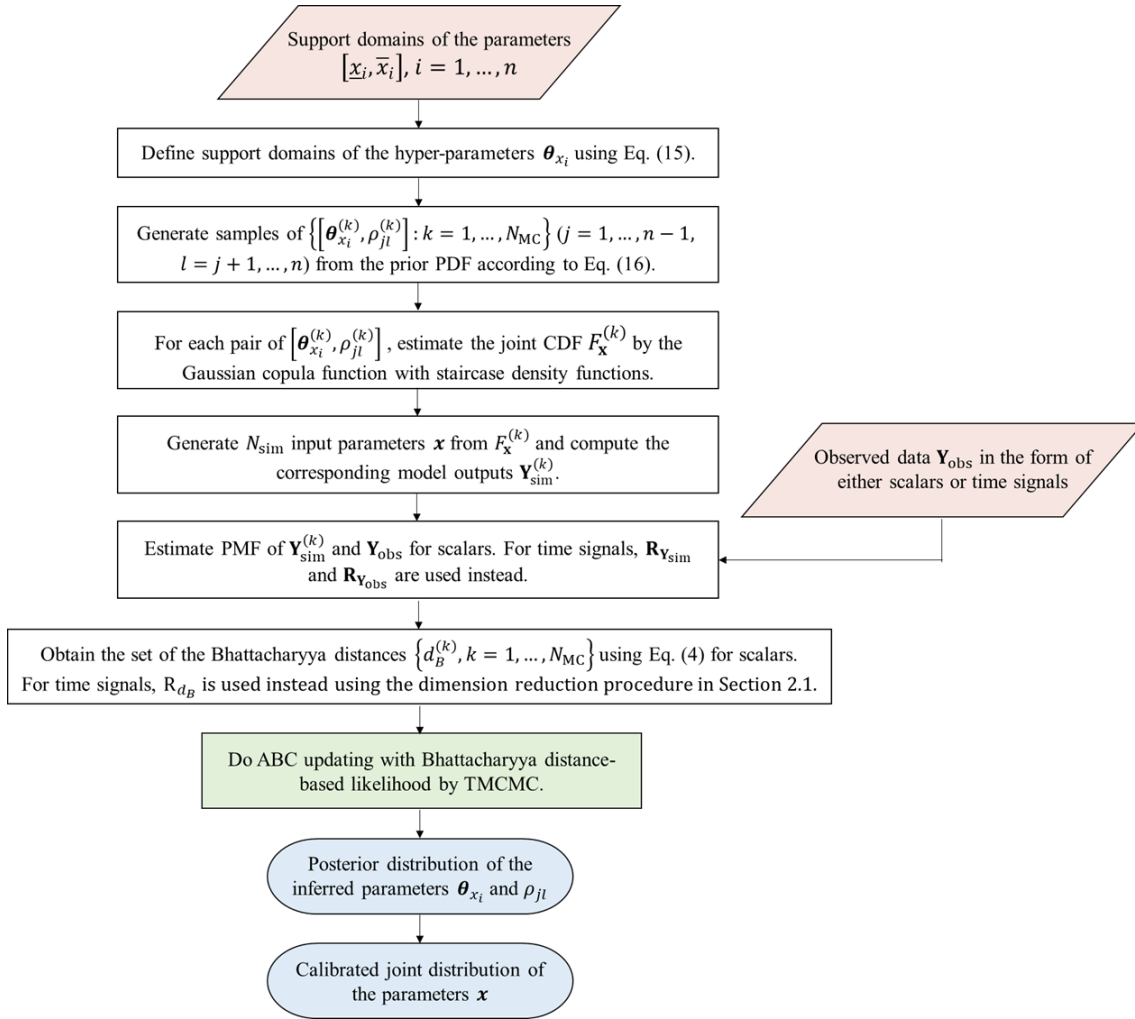
258 where  $P(\mathbf{Y}_{\text{obs}}^{(k)}|\boldsymbol{\vartheta})$  means the PDF value of the  $k$ th observations  $\mathbf{Y}_{\text{obs}}^{(k)}$  conditional to each instance of the  
 259 inferred parameters  $\boldsymbol{\vartheta}$ . The direct evaluation of Eq. (17), however, is often impractical since it requires  
 260 the significant number of model evaluations so as to precisely estimate the PDFs of the corresponding  
 261 model outputs.

262 The ABC method [12,13] has been successfully employed to overcome this obstacle by replacing  
 263 the above full likelihood function with an approximate but efficient likelihood function that contains  
 264 information of both the measurements and inferred parameters  $\boldsymbol{\vartheta}$ . Various forms of the approximate  
 265 likelihood functions have been investigated in the literature, such as the Gaussian [31], Epanechnikov  
 266 [32], and inverse squared error [33] functions. Regardless of the function form, it is essential to utilize  
 267 the comprehensive UQ metric which can serve as an effective connection between the measurements  
 268 and inferred parameters. In this study, an approximate likelihood function by the Gaussian function  
 269 is defined by utilizing the Bhattacharyya distance-based UQ metric as:

$$P_L(\mathbf{Y}_{\text{obs}}|\boldsymbol{\vartheta}) \propto \exp\left\{-\frac{d_B^2}{\varepsilon^2}\right\} \quad (18)$$

270 where  $\varepsilon$  is the pre-defined width factor, which controls the centralization degree of the posterior PDF.  
 271 A smaller  $\varepsilon$  provides a more peaked posterior PDF, which is more likely to converge to its true value  
 272 but needs more computation cost for convergence. Hence, its choice is based on specific applications,  
 273 while it is recommended to be within the interval of  $[10^{-3}, 10^{-1}]$  [31]. By utilizing the Bhattacharyya  
 274 distance (or the RMS value  $R_{dB}$  for the time signals case), the proposed likelihood enables to quantify  
 275 the comprehensive uncertainty characteristics of the model outputs and measurements.

276 The schematic in Fig. 1 illustrates overall framework of the proposed distribution-free stochastic  
 277 updating procedure. As already mentioned, only the support domains of the parameters are required  
 278 to perform this framework. Sampling from the prior PDF in Eq. (16) can be achieved by the rejection  
 279 sampling. TMCMC is then utilized to update the inferred parameters to the posterior PDF using the  
 280 Bhattacharyya distance-based approximate likelihood. By assigning most probable values (MPVs) of  
 281 the posterior PDF, the joint probabilistic distribution of the input parameters is finally calibrated such  
 282 that the stochastic model outputs generated from the joint distribution is capable to recreate wholly  
 283 the uncertainty characteristics of the target measurements. It is important to note that, the calibrated  
 284 distribution of the parameters is not necessarily applicable to the reliability analysis so as to estimate  
 285 the probabilities of rare events, since the parameters are finitely bounded due to the definition of the  
 286 staircase density functions and a domain where the rare event happens might be excluded.



287 **Fig. 1.** Schematic of the proposed stochastic model updating framework.  
 288

## 289 4. Principle and illustrative applications

### 290 4.1. Case study I: The two degree of freedom shear building model

291 The first case study is performed on a two degree of freedom (DOF) shear building model given  
 292 in Fig. 2(a). This case study aims at demonstrating the feasibility of the proposed updating procedure  
 293 for illustrative bivariate case, and how the stochastic model updating fails by ignoring the parameter  
 294 dependency. This model has been initially introduced by Ref. [28], where the first and second story  
 295 masses are considered as the fixed values with  $m_1 = 16.531 \times 10^3$  kg and  $m_2 = 16.131 \times 10^3$  kg. On  
 296 the other hand, the first and second interstory stiffnesses are characterized as  $k_1 = \bar{k}x_1$  and  $k_2 = \bar{k}x_2$ ,  
 297 where  $x = [x_1, x_2]$  indicates the inferred parameters, and  $\bar{k} = 29.7 \times 10^6$  N/m is the nominal value.



298 In Ref. [28], the prior PDF  $P(\mathbf{x})$  is determined by the pair of uncorrelated lognormal distributions  
 299 with the MPVs 1.3 and 0.8 for  $x_1$  and  $x_2$ , respectively, and the unit standard deviations. By employing  
 300 the first two natural frequencies  $\tilde{f}_1 = 4.31$  Hz and  $\tilde{f}_2 = 9.83$  Hz as the observed features, the posterior  
 301 PDF  $P(\mathbf{x}|\mathbf{Y}_{\text{obs}})$  is expressed as:

$$P(\mathbf{x}|\tilde{f}_1, \tilde{f}_2) \propto \exp\left[-\frac{M(\mathbf{x})}{2\sigma^2}\right]P(\mathbf{x}) \quad (19)$$

302 where  $\sigma = 1/16$  indicates the standard deviation of the prediction error;  $M(\cdot)$  is the modal measure-  
 303 of-fit function expressed as:

$$M(\mathbf{x}) = \sum_{j=1}^2 \lambda^2 \left[ \frac{f_j^2(\mathbf{x})}{\tilde{f}_j^2} - 1 \right]^2 \quad (20)$$

304 where  $\lambda = 1$  is the weight;  $f_j(\mathbf{x})$  denotes the  $j$ th natural frequency obtained as the model output. Fig.  
 305 2(b) illustrates the posterior distribution in Eq. (19). It can be seen that the posterior distribution has  
 306 a clear negative correlation.

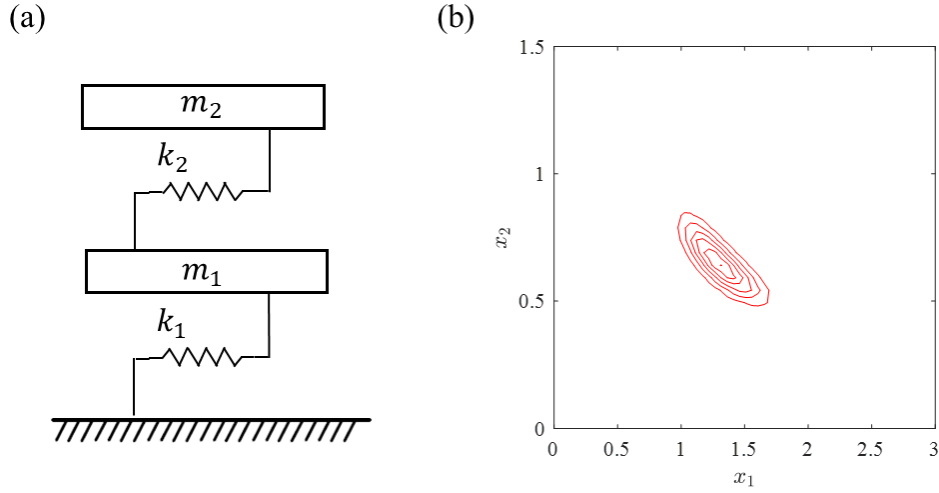


Fig. 2. (a) 2-DOF shear building model; (b) Posterior distribution in Eq. (19).

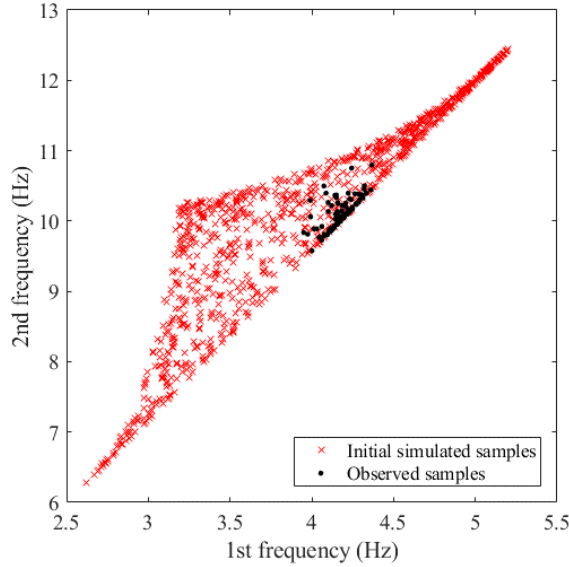
307  
 308 The aforementioned original problem can be interpreted to aim at estimating the set of plausible  
 309 values of the input parameters  $\mathbf{x}$  using the single set of observed features  $[\tilde{f}_1, \tilde{f}_2]$  through the Bayesian  
 310 scheme. Comparatively, the uncertainty characteristics of the input parameters and observed features  
 311 are altered hereafter to perform the stochastic updating where the joint probability distribution of the  
 312 input parameters,  $F_{\mathbf{x}}(\mathbf{x})$ , is calibrated using the multiple sets of the observed features. The target joint  
 313 distribution is defined to be identical to the posterior distribution in Eq. (19). The number of observed  
 314 features is set to be  $N_{\text{obs}} = 100$ ; thus,  $N_{\text{obs}}$  sample sets of the input parameters are generated from the  
 315 target distribution  $P(\mathbf{x}|\tilde{f}_1, \tilde{f}_2)$  utilizing TMCMC, and the corresponding observed features  $\mathbf{Y}_{\text{obs}}$  are  
 316 collected by evaluating the model with these sample sets. Note that the target distribution of the input  
 317 parameters is unknown beforehand in actual. As such, the altered problem is aimed at calibrating the  
 318 joint distribution of the input parameters to recreate wholly the uncertainty characteristics of  $\mathbf{Y}_{\text{obs}}$  by  
 319 the model outputs generated from the joint distribution.  
 320

321 The bounded support domains of  $x_1$  and  $x_2$  are determined as provided in Table 2. The support  
 322 domain of the hyper-parameters  $\theta_{x_1}$  and  $\theta_{x_2}$  can be computed using Eq. (15). Let the sample size be  
 323  $N_{\text{MC}} = 1000$ ,  $N_{\text{MC}}$  sets of the initial values of  $\theta_{x_1}$  and  $\theta_{x_2}$ , maintaining the moment constraints  $\Theta_1$  and  
 324  $\Theta_2$ , are generated by the rejection sampling while  $N_{\text{MC}}$  initial values of the correlation coefficient  $\rho_{12}$   
 325 are arbitrary generated from its support of  $[-1, 1]$ . For each set of  $[\theta_{x_1}, \theta_{x_2}, \rho_{12}]$ , the joint probability  
 326 distribution of the input parameters  $\mathbf{x}$  described by the Gaussian copula function with the marginal  
 327 staircase density functions is determined. The number of bins in staircase density estimation is chosen  
 328 as  $n_b = 25$ . At the same time, the number of simulated features is set to be  $N_{\text{sim}} = 1000$ ; hence,  $N_{\text{sim}}$   
 329 sample sets of the input parameters  $\mathbf{x}$  are generated from each joint distribution  $\{F_{\mathbf{x}}^{(k)}: k = 1, \dots, N_{\text{MC}}\}$ .

330 The corresponding initial simulated features  $\mathbf{Y}_{\text{sim}}^{(k)}$  are then collected by evaluating the model for each  
 331 sample sets of the input parameters. Arbitrary selected initial simulated features are plotted in Fig. 3,  
 332 together with the target observed features. The figure clearly demonstrates the presence of significant  
 333 discrepancy between the simulated and observed features, implying the necessity of stochastic model  
 334 updating for better representation of the uncertainty characteristics of the observed features by means  
 335 of the model outputs.

336 **Table 2.** Uncertainty characteristics of the 2-DOF model.

Parameter	Support domain	Target distribution
$x_1$	$x_1 \in [0, 3.0]$	The marginal distribution of Eq. (19)
$x_2$	$x_2 \in [0, 1.5]$	The marginal distribution of Eq. (19)

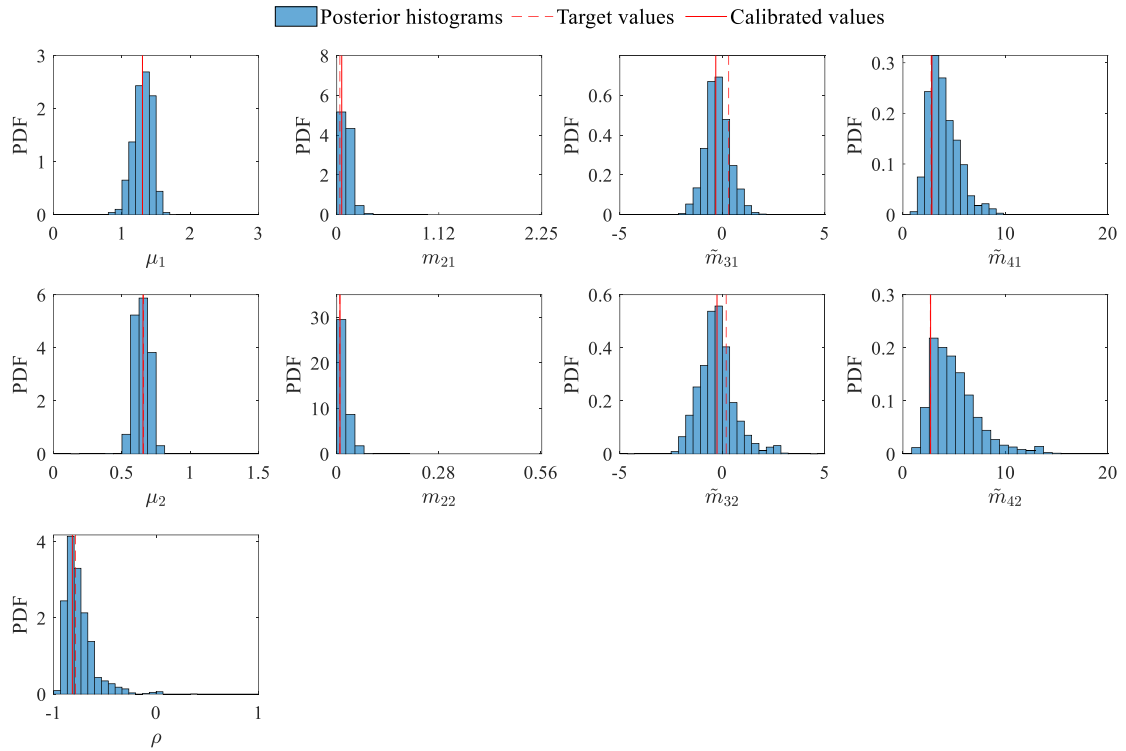


337 **Fig. 3.** Observed and initial simulated features.  
 338

339 The Bhattacharyya distance is estimated for each set of the simulated features  $\mathbf{Y}_{\text{sim}}^{(k)}$ . The number  
 340 of bins in the binning algorithm is chosen to be  $n_{\text{bin}} = 5$ . Then, the Bayesian model updating of totally  
 341 nine inferred parameters (i.e., the hyper-parameters  $\theta_{x_i} = \{\mu_i, m_{2i}, \tilde{m}_{3i}, \tilde{m}_{4i}\}$ , for  $i = 1, 2$ , as well as the  
 342 correlation coefficient  $\rho_{12}$ ) is performed using the Bhattacharyya distance-based likelihood function.  
 343 The width factor in the likelihood function is set to be  $\varepsilon = 0.02$ .

344 Fig. 4 shows the posterior PDFs of all the inferred parameters obtained after totally ten TMCMC  
 345 iterations, together with their target and calibrated values. The target values are estimated based on  
 346 samples generated from the target joint distribution, while the calibrated values are estimated as the  
 347 MPVs of the posterior PDFs. These values are summarized in Table 3. It can be seen that the posterior  
 348 PDFs of all the inferred parameters are significantly updated compared with their uniform priors that  
 349 are identical to ranges of the horizontal axes of Fig. 4. The posterior supports of the skewnesses and  
 350 kurtoses are, however, not reduced much from their prior supports, compared with the means and  
 351 variances, fulfilling the general experience that the higher order moments are difficult to be precisely  
 352 updated compared with the means [34,35]. Nevertheless, the calibrated values including the kurtoses  
 353 and the correlation coefficient are in good agreement with their target values with the largest relative  
 354 error less than 6 %, except for the variance  $m_{21}$  and two skewnesses  $\tilde{m}_{31}$  and  $\tilde{m}_{32}$ . The relative errors  
 355 are shown as percentages in the parentheses after the calibrated values in Table 3. It is noted that, the  
 356 large relative error in  $m_{21}$  can be explained to be caused by its quite small target value, and the error  
 357 is acceptable to obtain the staircase density function approximating the target distribution as shown  
 358 in Fig. 5. Meanwhile, the large errors in  $\tilde{m}_{31}$  and  $\tilde{m}_{32}$  are apparently caused by the wrongly identified  
 359 signs, whereas their absolute values are close to those of the targets. It should be noted that, the signs  
 360 of the skewnesses do not strongly affect the uncertainty characteristics of the output features as long  
 361 as their absolute values are small such that the resultant distributions are almost symmetric. To this  
 362 end, it is demonstrated that the Bhattacharyya distance can quantify not only mean information but

363 also higher statistical information, i.e., the variances, skewnesses, and kurtoses as well as correlation  
 364 coefficient.



365 **Fig. 4.** Posterior PDFs of the inferred parameters.

366 **Table 3.** Calibrated parameters of the 2-DOF model.

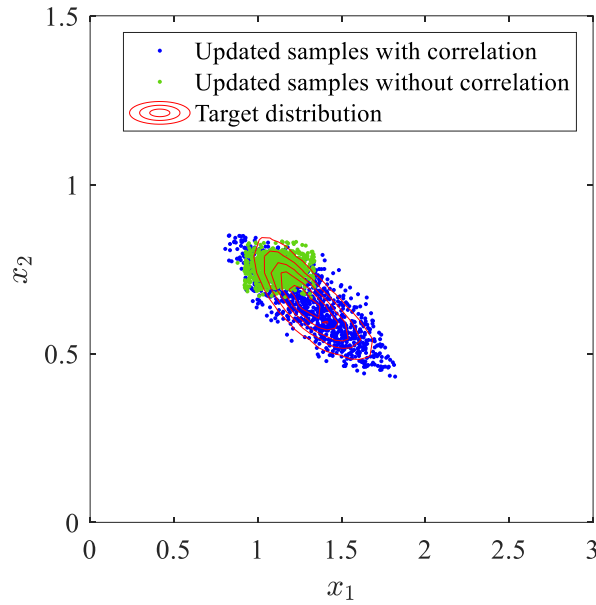
367

Parameter	Target value	Calibrated value	Calibrated value without correlation
$\mu_1$	1.3007	1.3000 (-0.05 %)	1.1214 (-13.78 %)
$m_{21}$	0.0348	0.0550 (48.85 %)	0.0157 (-54.89 %)
$\tilde{m}_{31}$	0.3102	-0.3200 (-203.16 %)	0.0022 (-99.29 %)
$\tilde{m}_{41}$	2.7503	2.8300 (2.90 %)	2.2912 (-16.69 %)
$\mu_2$	0.6568	0.6540 (-0.43 %)	0.7474 (13.79 %)
$m_{22}$	0.0085	0.0090 (5.88 %)	0.0031 (63.53 %)
$\tilde{m}_{32}$	0.1866	-0.1780 (-195.39 %)	-0.0849 (-145.50 %)
$\tilde{m}_{42}$	2.6679	2.7000 (1.20 %)	2.4355 (-8.71 %)
$\rho_{12}$	-0.7858	-0.8172 (-4.00 %)	–

368 To further demonstrate the results, the sample sets of the input parameters  $\mathbf{x}$  are generated from  
 369 the calibrated joint distribution (i.e., the Gaussian copula function with the marginal staircase density  
 370 functions) and are illustrated in Fig. 5. It can be seen that the samples generated from the calibrated  
 371 distribution shows good agreement with the target distribution. Meanwhile, the Bayesian updating  
 372 of only the marginal staircase density functions is also performed to demonstrate how the stochastic  
 373 model updating fails by ignoring the parameter dependency. The calibrated values of all the hyper-  
 374 parameters are listed in the last column of Table 3. Most of the parameters denote quite large relative  
 375 errors compared with those estimated with considering the parameter dependency. The sample sets  
 376 of the input parameters  $\mathbf{x}$  generated from the calibrated uncorrelated staircase density functions are  
 377 also plotted in the figure, which are only distributed in a part of the target distribution, implying the  
 378 importance of considering the parameter dependency in stochastic model updating.

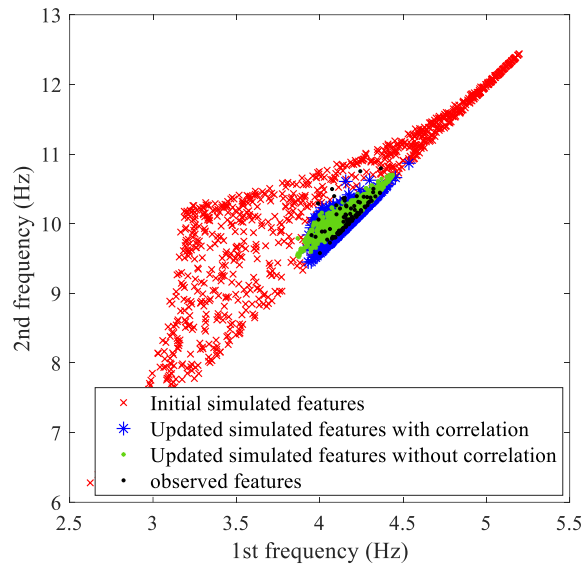
379 Finally, Fig. 6 illustrates the updated simulated features of  $f_1$  and  $f_2$  that is obtained by assigning  
 380 the calibrated joint distribution to  $\mathbf{x}$ , together with the initial simulated and target observed features.  
 381 Moreover, the simulated features are also computed for the case ignoring the parameter dependency,  
 382 and are provided in the figure. It can be seen that the updated simulated features show a distribution  
 383 equivalent to the observed features for both cases with and without the parameter dependency, while  
 384 the former provides better results. It implies that the Bhattacharyya distance metric has a potential to

385 recreate wholly the distribution of the target observed features regardless of the consideration of the  
 386 parameter dependency. Nonetheless, these results emphasize the importance of consideration of the  
 387 parameter dependency in the stochastic model updating, because even though the observed features  
 388 can be ideally quantified, the incompletely calibrated joint distribution of the input parameters could  
 389 result in an inaccurate prediction of other quantity of interests, which might be important for the risk  
 390 assessment or design optimization of the target structure.



391  
 392

**Fig. 5.** Updated samples of the input parameters.



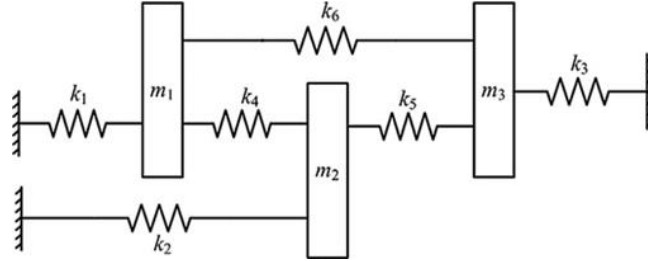
393  
 394

**Fig. 6.** Updated simulated features.

#### 395 4.2. Case study II: The three degree of freedom spring-mass system

396 The next case study is performed on a 3-DOF spring-mass system illustrated in Fig. 7. This case  
 397 study aims at demonstrating the capability of the proposed updating procedure for multivariate case.  
 398 This numerical system has been employed for demonstrating various stochastic updating techniques  
 399 [5,11], however, the uncertainty characteristics of the system are changed in this study to demonstrate  
 400 the proposed approach. The stiffness coefficients  $k_1$ ,  $k_2$ , and  $k_3$  are considered as the uncertain input  
 401 parameters to be calibrated, whereas the remaining parameters (i.e.  $k_4$  to  $k_6$  and the three masses  $m_1$   
 402 to  $m_3$ ) are treated to be the deterministic values:  $k_{4-6} = 5.0$  N/m,  $m_1 = 0.7$  kg,  $m_2 = 0.5$  kg, and  $m_3 =$

403 0.3 kg. The first three natural frequencies  $f_1$ ,  $f_2$ , and  $f_3$  are employed as the target output features the  
 404 uncertainty characteristics of which are driven by the joint probabilistic distribution of  $k_1$ ,  $k_2$ , and  $k_3$   
 405 that is assumed to be a correlated tri-variate Gaussian distribution. The given support domains of  $k_1$ ,  
 406  $k_2$ , and  $k_3$  and the target values of both the hyper-parameters and correlation coefficients are shown  
 407 in Table 4. It is noted that the support domains are set to cover more than 99.99 % confidence intervals  
 408 of the target marginal distributions. Such notification is important because the support domain of the  
 409 target joint distribution is not bounded, differently from the initial case study.



410  
411  
412

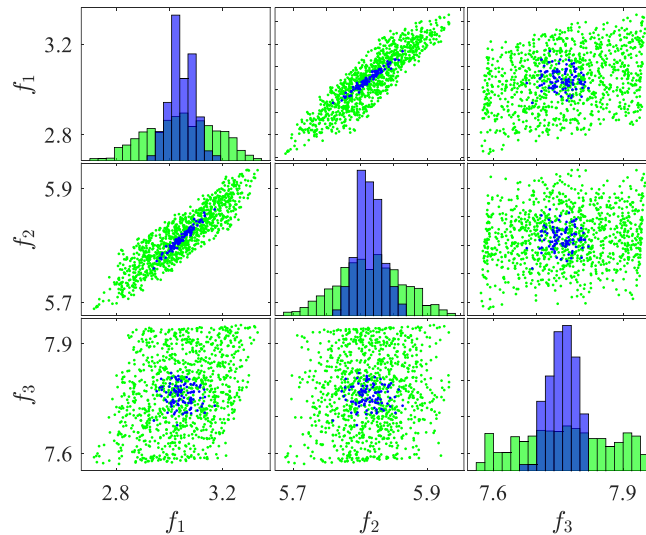
Fig. 7. 3-DOF spring-mass system.

Table 4. Uncertainty characteristics of the 3-DOF system.

Parameter	Support domain	Target distribution
$k_1, k_2, k_3$	$k_1 \in [2.5, 5.5]$ , $k_2 \in [4.5, 5.5]$ , $k_3 \in [5, 7]$	Gaussian, $\mu_1 = 4.0$ , $\mu_2 = 5.0$ , $\mu_3 = 6.0$ , $m_{21} = 0.09$ , $m_{22} = 0.01$ , $m_{23} = 0.04$ , $\rho_{12} = 0$ , $\rho_{13} = -0.6$ , $\rho_{23} = 0.6$
$k_4-k_6, m_1-m_3$	Deterministic	-

413 Consider the number of observed features be  $N_{\text{obs}} = 500$ ,  $N_{\text{obs}}$  sample sets of  $k_1$ ,  $k_2$ , and  $k_3$  are  
 414 generated from the target joint distribution and then the corresponding observed features  $\mathbf{Y}_{\text{obs}}$ , which  
 415 comprise  $f_1$ ,  $f_2$ , and  $f_3$ , are collected by evaluating the model with these sample sets.

416 On the other hand, let the sample size be  $N_{\text{MC}} = 1000$ ,  $N_{\text{MC}}$  sets of the initial values of the hyper-  
 417 parameters  $\theta_{k_1}$ ,  $\theta_{k_2}$ , and  $\theta_{k_3}$  and the correlation coefficients  $\rho_{12}$ ,  $\rho_{13}$ , and  $\rho_{23}$ , satisfying the moment  
 418 constraints  $\theta_1$ ,  $\theta_2$ , and  $\theta_3$  and the correlation coefficient constraint  $\mathcal{P}$ , are generated by the rejection  
 419 sampling in the support domains. For each set of the hyper-parameters and correlation coefficients,  
 420 the joint distribution of the three stiffness parameters described by the Gaussian copula function with  
 421 the marginal staircase density functions is determined. The number of bins  $n_b$  is set as the same value  
 422 as that in the first case study. The number of simulated features is set to be  $N_{\text{sim}} = 1000$ , so that totally  
 423  $N_{\text{sim}}$  sample sets of  $k_1$ ,  $k_2$ , and  $k_3$  are generated from each joint distribution. Then, the corresponding  
 424 initial simulated features are collected by evaluating the model for each sample sets. Fig. 8 compares  
 425 the histograms and scatters between the observed features and arbitrary chosen simulated features.



426  
427

Fig. 8. Observed features in blue and initial simulated features in green, with the unit in Hz.

428 The Bhattacharyya distance is estimated for each set of the initial simulated features. The number  
 429 of bins  $n_{\text{bin}}$  is chosen as the same value as that in the first case study. Then, the Bayesian updating of  
 430 in total 15 inferred parameters, i.e.,  $\theta_{k_i} = \{\mu_i, m_{2i}, \tilde{m}_{3i}, \tilde{m}_{4i}\}$ , for  $i = 1, 2, 3$ , and  $\rho_{ij}$ , for  $i = 1, 2$  and  $j =$   
 431  $i + 1, 3$ , is performed using the Bhattacharyya distance-based likelihood function. The width factor  $\varepsilon$   
 432 is set to be  $\varepsilon = 0.01$ .

433 By employing in total 17 TMCMC iterations, all the inferred parameters are well updated to the  
 434 posterior PDFs. The calibrated values (i.e., the MPVs of the posterior PDFs) of all inferred parameters  
 435 are presented in Table 5, together with the corresponding target values. The relative estimation errors  
 436 are also provided in the parentheses after the calibrated values. Note that the errors are not provided  
 437 for the skewnesses and the correlation coefficient  $\rho_{12}$  because their true values are zero. It can be seen  
 438 that the calibrated values of the mean and variance parameters are in good agreement with the target  
 439 values with the largest relative error less than 5 %. On the contrary, the skewness parameters exhibit  
 440 differences compared with their target values, especially for  $\tilde{m}_{31}$ . However, the calibrated values are  
 441 small enough for resulting in almost symmetric distributions as similar as the target distributions, as  
 442 depicted in Fig. 9. The kurtosis parameters also exhibit large errors compared with their target values,  
 443 whereas these errors are also permissible to obtain reasonable distributions compared with the target  
 444 distributions as illustrated in Fig. 9. As such, both the skewness and kurtosis parameters are relatively  
 445 insensitive to the uncertainty characteristics of the target output features, compared with the means  
 446 and variances. Note that, it does not, however, mean that such higher order moment parameters are  
 447 always insensitive to the results. As a matter of fact, in the previous example, the kurtosis parameters  
 448 are precisely updated, implying they are sensitive to the target output features in that example. More  
 449 importantly, all correlation coefficients are in good agreement with their target values with the largest  
 450 relative error around 10 %, implying that the proposed procedure is capable to properly capture the  
 451 correlation structure regardless of no, negative, and positive correlations.

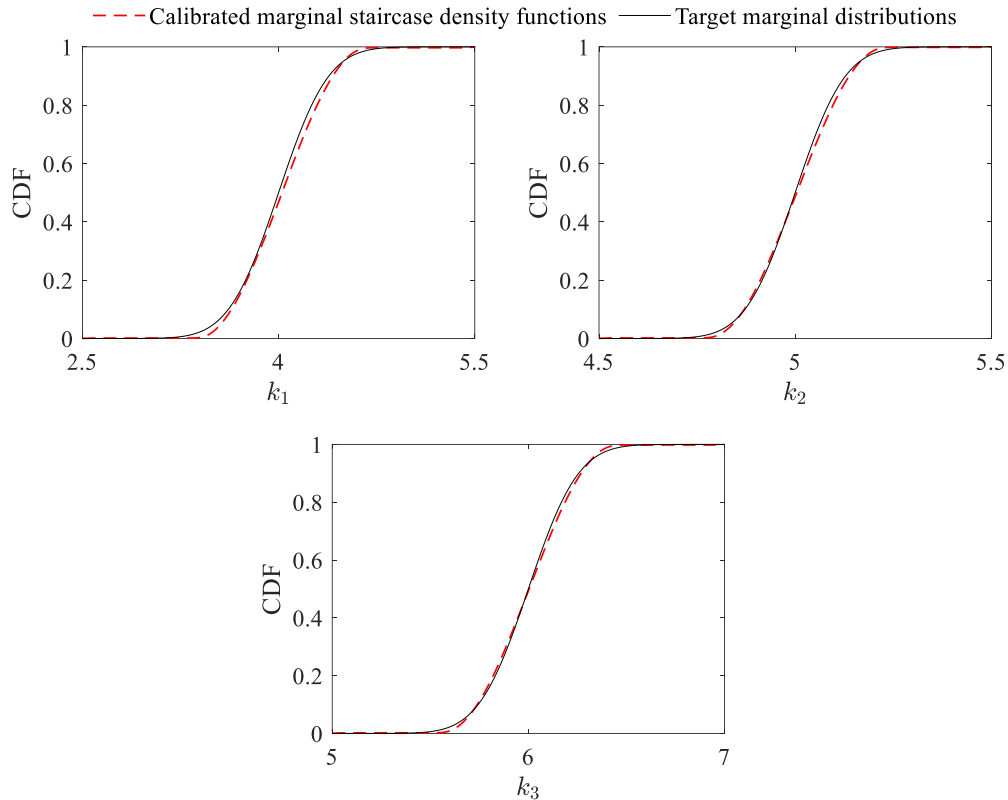
452

**Table 5.** Calibrated parameters of the 3-DOF system.

Parameter	Target value	Calibrated value
$\mu_1$	4.0	4.0286 (0.72 %)
$m_{21}$	0.09	0.0890 (-1.11 %)
$\tilde{m}_{31}$	0	0.2220
$\tilde{m}_{41}$	3.0	4.4400 (48.00 %)
$\mu_2$	5.0	5.0035 (0.07 %)
$m_{22}$	0.01	0.0104 (4.00 %)
$\tilde{m}_{32}$	0	-0.0500
$\tilde{m}_{42}$	3.0	3.8100 (27.00 %)
$\mu_3$	6.0	6.0030 (0.05 %)
$m_{23}$	0.04	0.0410 (2.50 %)
$\tilde{m}_{33}$	0	-0.0214
$\tilde{m}_{43}$	3.0	3.9400 (31.33 %)
$\rho_{12}$	0	-0.0058
$\rho_{13}$	-0.6	-0.5728 (4.53 %)
$\rho_{23}$	0.6	0.5398 (10.03 %)

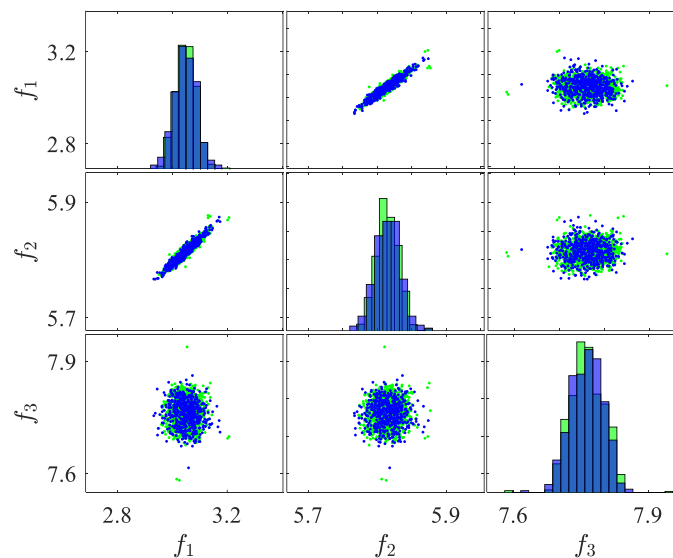
453 The joint distribution of  $k_1$ ,  $k_2$ , and  $k_3$  is then obtained as the Gaussian copula function having  
 454 the marginal staircase density functions, assigned the calibrated values of the hyper-parameters and  
 455 correlation coefficients. Fig. 9 shows the marginal CDF of each stiffness, along with the corresponding  
 456 target marginal distribution. It is noted that, since the marginal distributions are obtained as staircase  
 457 (i.e., discrete) density functions, the CDFs are estimated from the samples generated according to the  
 458 staircase density functions, via the kernel density estimation. As can be seen, the estimated staircase  
 459 density functions are in good agreement with their target marginal distribution, which supports that  
 460 the aforementioned estimate errors in the skewness and kurtosis parameters are within an allowance  
 461 for calibrating the joint distribution of the parameters. Nevertheless, it is noted that, in the tail regions,  
 462 the calibrated distributions, in particular for  $k_1$ , remain discrepancy from the target distribution due  
 463 to the estimate errors in the kurtosis parameters, while the discrepancy in the tail regions do not affect  
 464 much the model outputs as illustrated in Fig. 10. Moreover, the obtained distributions have bounded

465 support domains which are identical to ranges of the horizontal axes of Fig. 9 because of the definition  
 466 of the staircase density functions, whereas the target Gaussian distributions do not have the bounded  
 467 supports. It implies that the proposed procedure does not limit its applicability to the case where the  
 468 investigated parameters have bounded supports, however, at the same time, it also indicates that the  
 469 calibrated joint distribution cannot be employed for reliability analysis, where the target is estimating  
 470 the probabilities of rare events that can be occurred out of the support domains. It is noted that, this  
 471 limitation does not prevent the use of the proposed procedure in the stochastic model updating, since  
 472 the main motivation of the stochastic model updating is to obtain the model that is capable to describe  
 473 the system of interest conditioned on the observed data whereas reliability analysis is only one of the  
 474 potential usages of the calibrated model.



475  
 476

**Fig. 9.** Calibrated marginal distributions of the input parameters.



477  
 478

**Fig. 10.** Observed features in blue and updated simulated features in green, with the unit in Hz.

479 Finally, Fig. 10 compares the histograms and scatters between the target and updated simulated  
 480 features. Compared with the initial simulated features in Fig. 8, It can be seen that the uncertainties  
 481 in the three stiffness parameters are correctly calibrated by the proposed procedure and the calibrated  
 482 model is capable to recreate wholly the uncertainty characteristics of the observed features. As such,  
 483 the relatively large estimate errors in the higher order moment parameters are permissible, since the  
 484 objective of the proposed method is not to estimate the individual moment parameters precisely but  
 485 rather to obtain model outputs that are identical to the observed data, to which some higher moment  
 486 parameters could be insensitive.

## 487 5. Nonlinear dynamic system updating

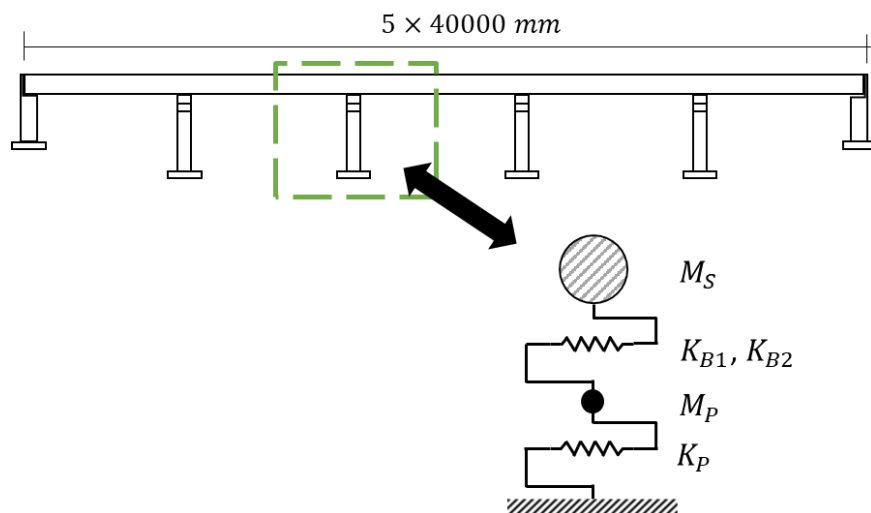
### 488 5.1. Problem description

489 The proposed approach is further demonstrated on the updating of nonlinear dynamic systems  
 490 using the measured time signals. For this purpose, a model updating problem of a reinforced concrete  
 491 (RC) bridge pier using simulated seismic response data is investigated. The target bridge is a seismic-  
 492 isolated bridge with lead rubber bearings, designed based on the specifications for highway bridges  
 493 in Japan [36]. Its structural descriptions are detailed in Table 6. Fig. 11 shows the 2-DOF lumped mass  
 494 model as the numerical model of the target structure, in which the two lumped masses represent the  
 495 superstructure and RC pier, and the two horizontal springs denote the rubber bearings and RC pier.  
 496 The boundary condition at the surface is assumed to be fixed. The nonlinearity of the rubber bearings  
 497 is characterized by a bilinear model with the ratio of the yield stiffness  $K_{B1}$  to the post-yield stiffness  
 498  $K_{B2}$  of 6.5:1 based on the manual on bearings for highway bridges in Japan [37]. Meanwhile, that of  
 499 the RC pier is characterized by a bilinear model with the elastoplastic characteristic and the stiffness  
 500 degradation model, namely Takeda model [38]. The well-known Rayleigh damping model is utilized  
 501 as the damping model in which the damping ratios of the rubber bearings and RC pier are set to be  
 502 0 % and 2 %, respectively.

503

**Table 6.** Descriptions of the target bridge pier.

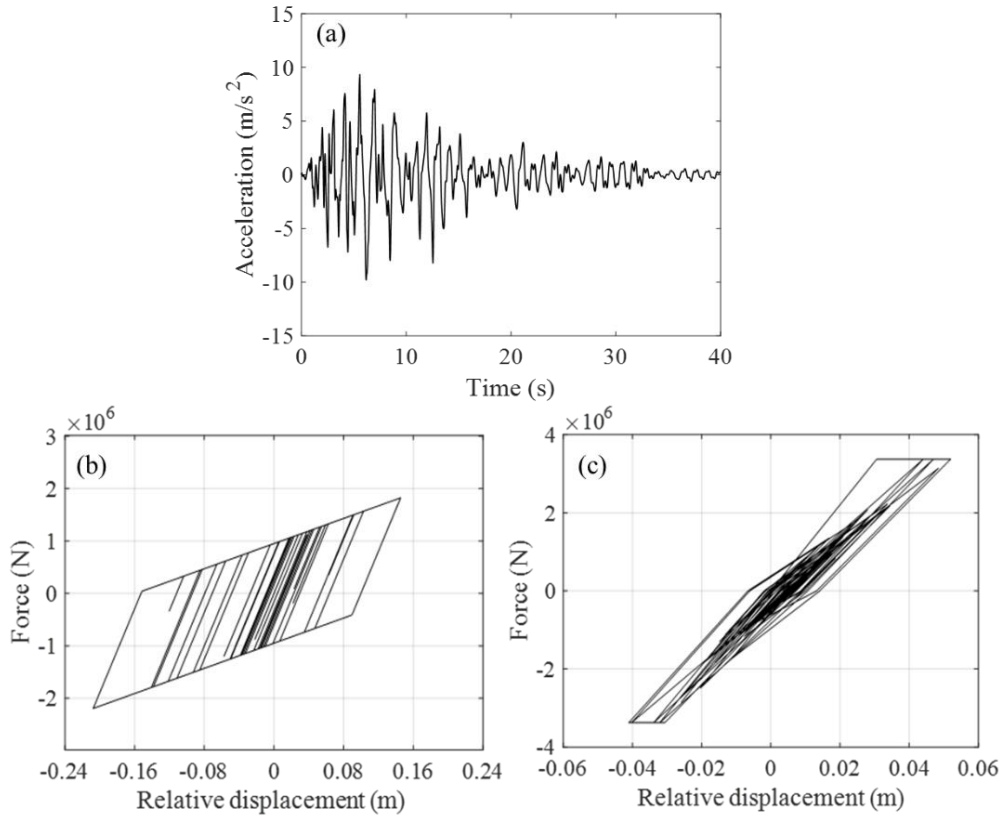
	Structural parameter	Nominal value
Superstructure	Mass $M_S$ (ton)	604.0
Rubber bearings	Yield strength (kN)	1118
	Yield stiffness $K_{B1}$ (kN/m)	40000
	Post-yield stiffness $K_{B2}$ (kN/m)	6000
RC pier	Mass $M_P$ (ton)	346.2
	Yield strength (kN)	3374
	Yield stiffness $K_P$ (kN/m)	110100
	Yield displacement (m)	0.0306

504  
505

**Fig. 11.** Numerical modeling of the target bridge pier.



506 The aim of this updating problem is to quantify the uncertainty characteristics of the post-yield  
 507 stiffness of the rubber bearings,  $K_{B2}$ , which governs the nonlinear behaviour of the target bridge pier  
 508 under strong earthquakes, as well as the remaining stiffnesses  $K_{B1}$  and  $K_P$ . These three stiffnesses are  
 509 parameterized as  $K_{B1} = \bar{K}_{B1}x_1$ ,  $K_{B2} = \bar{K}_{B2}x_2$ , and  $K_P = \bar{K}_P x_3$ , where  $\mathbf{x} = [x_1, x_2, x_3]$  are uncertain input  
 510 parameters, and  $\bar{K}_{B1}$ ,  $\bar{K}_{B2}$ , and  $\bar{K}_P$  are the nominal values shown in Table 6. The other parameters are  
 511 assumed to be fixed constants with the nominal values. The time-history of the acceleration response  
 512 at the superstructure subjected to the level-2 type-II-1 earthquake introduced in Ref. [36] is used as  
 513 the target output features. The duration time of the input ground motion is 40 s. Time history analysis  
 514 of the 2-DOF model is performed using the Newmark  $\beta$  method ( $\beta = 1/4$  and  $\gamma = 1/2$ ) with the time  
 515 step  $\Delta t = 0.001$  s. Fig. 12 illustrates the time-history of the acceleration response at the superstructure  
 516 and the force-displacement responses of the rubber bearings and pier for the case when all parameters  
 517 are fixed to the nominal values shown in Table 6.



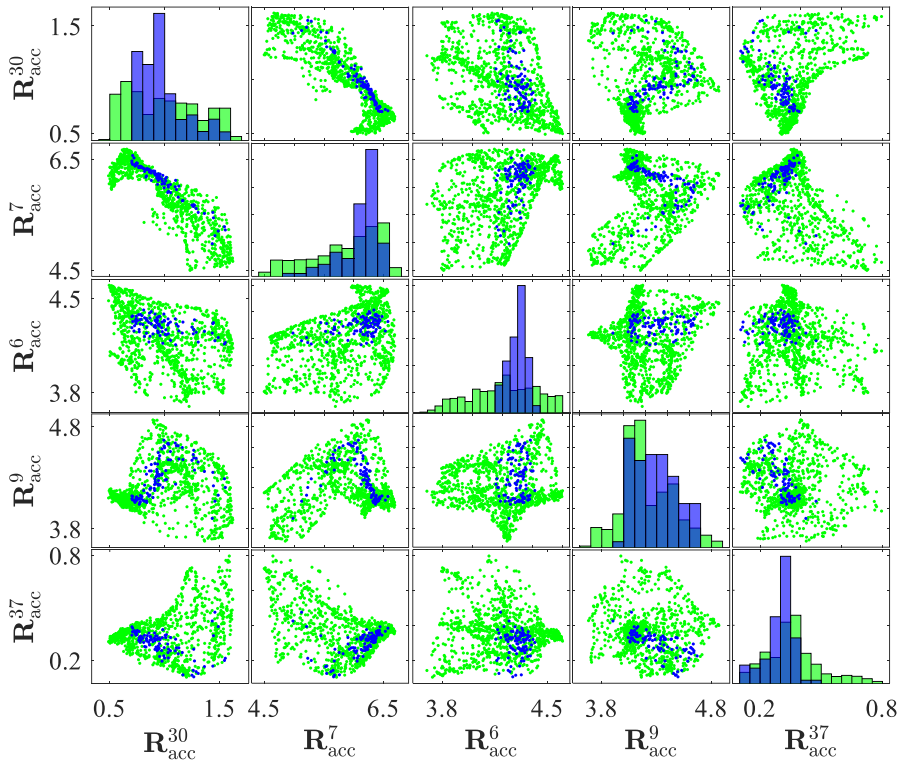
518 **Fig. 12.** (a) Time-history of the acceleration response at superstructure; (b) Force-displacement response of  
 519 rubber bearings; (c) Force-displacement response of RC pier.  
 520

521 The target joint distribution of the input parameters  $\mathbf{x}$  is considered to be a correlated tri-variate  
 522 Gaussian distribution, in which a positive correlation between  $x_1$  and  $x_2$  (i.e., between the initial and  
 523 post stiffnesses of the rubber bearings) is introduced. The pre-defined support domains of  $x_1, x_2,$  and  
 524  $x_3$  and the target values of the hyper-parameters and correlation coefficients are detailed in Table 7.  
 525 Similar to the previous case study, the support domains are determined to cover more than 99.99 %  
 526 confidence intervals of their target marginal distributions. Suppose the number of observed features  
 527 be  $N_{\text{obs}} = 100$ ,  $N_{\text{obs}}$  sample sets of the input parameters  $\mathbf{x}$  are generated according to the target joint  
 528 distribution and then the corresponding observed features  $\mathbf{Y}_{\text{obs}}$  of the time-history of the acceleration  
 529 response at the superstructure, are collected by evaluating the model with these sample sets.

530 **Table 7.** Uncertainty characteristics of the target bridge pier.

Parameter	Support set	Target distribution
$x_1, x_2, x_3$	$x_1 \in [0.7, 1.3], x_2 \in [0.7, 1.3],$ $x_3 \in [0.7, 1.3]$	Gaussian, $\mu_1 = 1.0, \mu_2 = 1.0, \mu_3 = 1.0, m_{21} = 0.0049,$ $m_{22} = 0.0049, m_{23} = 0.0049, \rho_{12} = 0.8, \rho_{13} = 0, \rho_{23} = 0$
$M_S, M_P$	Deterministic	–

531 In this example, totally 13 inferred parameters, i.e., the hyper-parameters  $\theta_{x_i} = \{\mu_i, m_{2i}, m_{3i}, m_{4i}\}$ ,  
 532 for  $i = 1, 2, 3$ , and correlation coefficient  $\rho_{12}$  is taken into account. Note that the remaining correlation  
 533 coefficients are assumed to be zero in advance and ignored in the updating procedure. Suppose the  
 534 sample size be  $N_{MC} = 100$ ,  $N_{MC}$  sets of the hyper-parameters maintaining the moment constraints  $\Theta_1$   
 535  $\Theta_2$ , and  $\Theta_3$ , are generated by the rejection sampling whereas  $N_{MC}$  sets of the correlation coefficient are  
 536 arbitrary generated from the support of  $[-1, 1]$ . For each set of  $[\theta_{x_1}, \theta_{x_2}, \theta_{x_3}, \rho_{12}]$ , the joint probability  
 537 distribution of the input parameters  $\mathbf{x}$  is defined as the Gaussian copula function having the marginal  
 538 staircase density functions. The number of bins  $n_b$  is chosen to be  $n_b = 50$ . The number of simulated  
 539 features, on the other hand, is set as  $N_{sim} = 500$ ; hence,  $N_{sim}$  sample sets of  $\mathbf{x}$  are generated from each  
 540 joint distribution  $\{F_x^{(k)}: k = 1, \dots, N_{MC}\}$ , and then the corresponding initial simulated features  $\mathbf{Y}_{sim}^{(k)}$  are  
 541 obtained by evaluating the model with these samples. The window length in the dimension reduction  
 542 procedure introduced in Section 2.1 is set to be  $L = 0.025(t + 1)$ , with  $t = 40/0.001 = 40000$ . Hence,  
 543 the RMS matrices of both the simulated and observed features,  $\mathbf{R}_{Y_{sim}^s}^{(k)}$  and  $\mathbf{R}_{Y_{sim}^s}$ , for  $\forall s = 1, \dots, 40$ , are  
 544 defined. Fig. 13 compares the histograms and scatters between the observed and simulated features  
 545 by employing five arbitrary selected RMS matrices of  $s = 30, 7, 6, 9, 37$ . The figure demonstrates that  
 546 the target features show strong nonlinearity, making the updating problem significantly challenging.  
 547 The Bhattacharyya distance is estimated for each pair of the simulated and observed RMS matrices,  
 548 and the RMS value of the Bhattacharyya distances,  $R_{dB}$ , is used as the UQ metric in the approximate  
 549 likelihood. The number of bins  $n_{bin}$  is chosen as  $n_{bin} = 10$  while the width factor  $\varepsilon$  is set as  $\varepsilon = 0.01$ .



550  
 551

Fig. 13. Observed features in blue and initial simulated features in green, with the unit in  $m/s^2$ .

## 552 5.2. Results assessment

553 By employing totally 13 TMCMC iterations, all the inferred parameters are well updated to the  
 554 posterior PDFs. The calibrated values of the inferred parameters are detailed in Table 8, together with  
 555 the corresponding target values. The relative estimation errors are also shown in the parentheses after  
 556 the calibrated values. The calibrated values of all mean parameters and the variance parameter  $m_{21}$   
 557 are in good agreement with the target values, while the remaining variance parameters exhibit large  
 558 estimate errors due to their quite small target values. In spite of the large relative errors, the calibrated  
 559 values of the variance parameters are close to the target values compared with the prior supports and

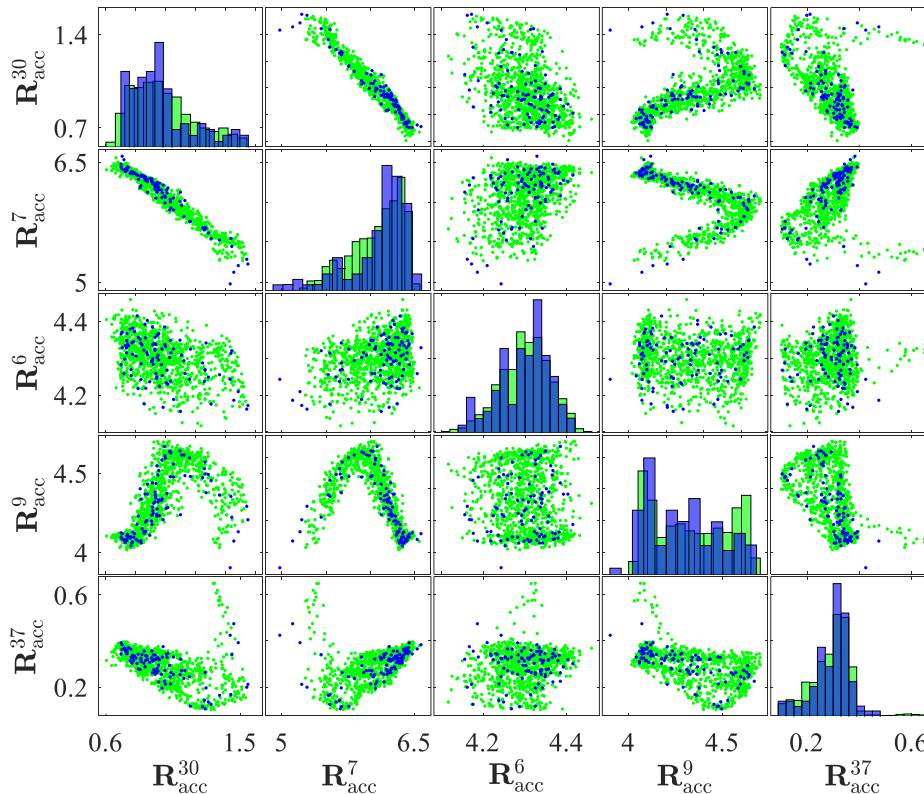
560 the errors are within an allowance to achieve the model outputs close to the observations. In addition,  
 561 the skewnesses and kurtoses exhibit differences compared with their target values, while these errors  
 562 are also within an allowance to achieve the model outputs close to the target observations, as similar  
 563 as the previous example. Moreover, the positive correlation induced is also captured by the proposed  
 564 procedure though a certain error is still remained compared with the target value. By assigning these  
 565 calibrated values, the joint distribution of  $\boldsymbol{x}$  is tuned identical to the target distribution.

566

**Table 8.** Calibrated parameters of the target bridge pier model.

Parameter	Target value	Calibrated value
$\mu_1$	1.0	0.9958 (-0.42 %)
$m_{21}$	0.0049	0.0045 (-4.44 %)
$\tilde{m}_{31}$	0	-0.1688
$\tilde{m}_{41}$	3.0	4.3450 (44.83 %)
$\mu_2$	1.0	0.9992 (-0.08 %)
$m_{22}$	0.0049	0.0065 (32.65 %)
$\tilde{m}_{32}$	0	0.4050
$\tilde{m}_{42}$	3.0	3.9500 (31.67 %)
$\mu_3$	1.0	0.9996 (-0.04 %)
$m_{23}$	0.0049	0.0068 (38.78 %)
$\tilde{m}_{33}$	0	-0.3025
$\tilde{m}_{43}$	3.0	4.3960 (46.53 %)
$\rho_{12}$	0.8	0.6736 (-15.80 %)

567 Finally, Fig. 14 compares the histograms and scatters between the target and simulated features  
 568 for the five arbitrary selected RMS matrices of  $s = 30, 7, 6, 9, 37$ . Compared with the initial simulated  
 569 features in Fig. 13, It can be seen the updated simulated features are identical to the observed features  
 570 capturing the complicated nonlinear structure. This indicates the feasibility of the proposed approach  
 571 in the stochastic model updating of nonlinear dynamic systems for recreating wholly the uncertainty  
 572 characteristics of the target measured time signals, even though the prior knowledge about the joint  
 573 probability distribution of the model parameters is extremely limited.



574  
 575

**Fig. 14.** Observed features in blue and updated simulated features in green, with the unit in  $m/s^2$ .

## 576 6. Conclusions

577 This paper presents three contributions for calibrating the joint probabilistic distribution of the  
578 correlated parameters through the stochastic model updating by a limited number of measurement  
579 data. First, each marginal distribution is characterized by staircase density functions and their hyper-  
580 parameters are subjected to be updated. The staircase density functions can flexibly describe a broad  
581 range of distributions; thus, no limiting hypotheses on the distribution families is required differently  
582 from the most of the stochastic model updating methods. Next, the dependence structure among the  
583 parameters are described by the Gaussian copula. The correlation coefficients are also subjected to be  
584 updated; thus, even the prior knowledge on the presence of parameter dependencies is not required.  
585 Finally, the Bhattacharyya distance-based UQ metric is proposed to define an approximate likelihood  
586 capable of quantifying the stochastic discrepancy between the model outputs and measurements. As  
587 such, the inferred parameters, i.e., the hyper-parameters and correlation coefficients are successfully  
588 updated through the Bayesian model updating. Two exemplary applications and followed nonlinear  
589 dynamic system updating problem demonstrate the feasibility of the proposed updating framework  
590 and the importance of considering the parameter dependency in the stochastic model updating.

591 However, open problems still exist. First, the cost function in the optimization problem solved  
592 for estimating the staircase density function is solely selected in this study. The staircase density that  
593 attains other optimality criteria, such as the maximal entropy, can be similarly formulated, but further  
594 studies are necessary to investigate the most suitable choice of the cost function for model updating.  
595 Second, the Gaussian copula might not be suitable if the parameters demonstrate a strong nonlinear  
596 dependency. The assumption on the copula function type introduces another source of uncertainty,  
597 i.e., the model bias, and such uncertainty should be quantified by, for instance, the Bayesian model  
598 class selection. These two challenges will be addressed in the future work.

## 599 Acknowledgments

600 The first author acknowledges the support of the Deutsche Forschungsgemeinschaft (DFG,  
601 German Research Foundation) — SFB1463-434502799.

## 602 References

- 603 1. J.E. Mottershead, M. Ling, M.I. Friswell, The sensitivity method in finite element model  
604 updating: A tutorial, *Mech. Syst. Signal Process.* 25 (2011) 2275-2296.
- 605 2. E. Patelli, Y. Govers, M. Broggi, H.M. Gomes, M. Ling, J.E. Mottershead, Sensitivity or  
606 Bayesian model updating: a comparison of techniques using the DLR AIRMOD test data.  
607 *Arch. Appl. Mech.* 87 (2017) 905-925.
- 608 3. J.E. Mottershead, M.I. Friswell, Model Updating In Structural Dynamics. *J. Sound Vib.* 167  
609 (1993) 347-375.
- 610 5. D. Shan, Q. Li, I. Khan, X. Zhou, A novel finite element model updating method based on  
611 substructure and response surface model, *Eng. Struct.* 103 (2015) 147-156.
- 612 6. C. Mares, J.E. Mottershead, M.I. Friswell, Stochastic model updating: Part 1—theory and  
613 simulated example, *Mech. Syst. Signal Process.* 20 (2006) 1674-1695.
- 614 7. K.K. Sairajan, G.S. Aglietti, Robustness of system equivalent reduction expansion process on  
615 spacecraft structure model validation, *AIAA J.* 50 (2012) 2376-2388.
- 616 8. S. Bi, S. Prabhu, S. Cogan, S. Atamturktur, Uncertainty quantification metrics with varying  
617 statistical information in model calibration and validation, *AIAA J.* 55 (2017) 3570-3583.
- 618 9. B. Goller, M. Broggi, A. Calvi, G.I. Schuëller, A stochastic model updating technique for  
619 complex aerospace structures, *Finite Elem. Anal. Des.* 47 (2011) 739-752.

- 620 10. Y. Govers, M. Link, Stochastic model updating—Covariance matrix adjustment from  
621 uncertain experimental modal data, *Mech. Syst. Signal Process.* 24 (2010) 696-706.
- 622 11. S. Bi, M. Broggi, M. Beer, The role of the Bhattacharyya distance in stochastic model updating,  
623 *Mech. Syst. Signal Process.* 117 (2019) 437-452.
- 624 12. M.A. Beaumont, W. Zhang, D.J. Balding, Approximate Bayesian computation in population  
625 genetics, *Genetics* 162 (2002) 2025-2035.
- 626 13. B.M. Turner, T. Van Zandt, A tutorial on approximate Bayesian computation, *J. Math. Psychol.*  
627 56 (2012) 69-85.
- 628 14. M. Kitahara, S. Bi, M. Broggi, M. Beer, Bayesian model updating in time domain with  
629 metamodel-based reliability method, *J. Risk Uncertainty Eng. Syst. Part A: Civ. Eng.* 7 (2021)  
630 04021030.
- 631 15. L.G. Crespo, S.P. Kenny, The NASA Langley multidisciplinary uncertainty quantification  
632 challenge, *Mech. Syst. Signal Process.* 152 (2021) 107405.
- 633 16. M. Kitahara, S. Bi, M. Broggi, M. Beer, Nonparametric Bayesian stochastic model updating  
634 with hybrid uncertainties, *Mech. Syst. Signal Process.* 163 (2022) 108195.
- 635 17. L.G. Crespo, S.P. Kenny, D.P. Giesy, B.K. Stanford, Random variables with moment-matching  
636 staircase density function, *Appl. Math. Model* 64 (2018) 196-213.
- 637 18. X.S. Tang, D.Q. Li, C.B. Zhou, K.K. Phoon, L.M. Zhang, Impact of copulas for modeling  
638 bivariate distributions on system reliability, *Struct. Safety* 44 (2013) 80-90.
- 639 19. D.Q. Li, L. Zhang, X.S. Tang, W. Zhou, J.H. Li, C.B. Zhou, K.K. Phoon, Bivariate distribution  
640 of shear strength parameters using copulas and its impact on geotechnical system reliability,  
641 *Compt. Geotech.* 68 (2015) 184-195.
- 642 20. X.S. Tang, D.Q. Li, C.B. Zhou, K.K. Phoon, Copula-based approaches for evaluating slope  
643 reliability under incomplete probability information, *Struct. Safety* 52 (2015) 90-99.
- 644 21. A. Bhattacharyya, On a measure of divergence between two multinomial populations, *Indian*  
645 *J. Stat.* 7 (1964) 401-406.
- 646 22. B.K. Patra, R. Launonen, V. Ollikainen, S. Nandi, A new similarity measure using  
647 Bhattacharyya coefficient for collaborative filtering in sparse data, *Knowledge-Based Syst.* 82  
648 (2015) 163-177.
- 649 23. R. Sharma, S. Devi, G. Kapoor, N.S. Barnett, A brief note on some bounds connecting lower  
650 order moments for random variables defined on a finite interval, *Int. J. Theor. Appl. Sci.* 1  
651 (2009) 83-85.
- 652 24. P. Kumar, Moment inequalities of a random variable defined over a finite interval, *J. Inequ.*  
653 *Pure. Appl. Math.* 3 (2002) 1-11.
- 654 25. R.B. Nelsen, *An Introduction to Copulas*; 2nd ed, Springer, New York, 2006.
- 655 26. L.H. Haff, Parameter estimation for pair-copula constructions, *Bernoulli* 19 (2013) 462-491.
- 656 27. J.L. Beck, L.S. Ktalygiotis, Updating models and their uncertainties. I: Bayesian statistical  
657 framework, *J. Eng. Mech.* 124 (1998) 455-461.
- 658 28. J.L. Beck, S.K. Au, Bayesian updating of structural models and reliability using Markov chain  
659 Monte Carlo simulation, *J. Eng. Mech.* 128 (2002) 380-391.
- 660 29. J. Ching, Y.C. Chen, Transitional Markov chain Monte Carlo method for Bayesian updating,  
661 model class selection, and model averaging, *J. Eng. Mech.* 133 (2007) 816-832.

- 662 30. W. Betz, I. Papaioannou, D. Straub, Transitional Markov chain Monte Carlo: Observations and  
663 improvements, *J. Eng. Mech.* 142 (2016).
- 664 31. E. Patelli, D.A. Alvarez, M. Broggi, M. de Angelis, Uncertainty management in  
665 multidisciplinary design of critical safety systems, *J. Aerosp. Inf. Syst.* 12 (2015) 140-169.
- 666 32. C. Safta, K. Sargsyan, H.N. Najm, K. Chowdhary, B. Debusschere, L.P. Swiler, M.S. Eldred,  
667 Probabilistic methods for sensitivity analysis and calibration in the NASA challenge problem,  
668 *J. Aerosp. Inf. Syst.* 12 (2015) 219-234.
- 669 33. R. Rocchetta, M. Broggi, Q. Huchet, E. Patelli, On-line Bayesian model updating for structural  
670 health monitoring, *Mech. Syst. Signal Process.* 103 (2018) 174-195.
- 671 34. P. Li, Z. Lu, Y. Zhao, Bayesian updating of time-dependent structural reliability using the  
672 method of moment, *J. Risk Uncertainty Eng. Syst. Part A: Civ. Eng.* 7 (2021) 04021066.
- 673 35. B. Liao, R. Zhao, K. Yu, C. Liu, A novel interval model updating framework based on  
674 correlation propagation and matrix-similarity method, *Mech. Syst. Signal Process.* 162 (2022)  
675 108039.
- 676 36. Japan Road Association, Design specifications of highway bridges V: Seismic design,  
677 Maruzen, Tokyo, 2016.
- 678 37. Japan Road Association, Manual on bearings for highway bridges, Maruzen, Tokyo, 2004. (In  
679 Japanese).
- 680 38. T. Takeda, M.A. Sozen, N.N. Nielsen, Reinforced concrete response to simulated earthquakes,  
681 *J. Struct. Div.* 96 (1970) 2257-2573.